



Short communication

Nanoporous titanium obtained from a spinodally decomposed Ti alloy



N.T. Panagiotopoulos^{a, b, c, *}, A. Moreira Jorge^{a, b}, I. Rebai^a, K. Georgarakis^{a, c},
W.J. Botta^{a, b}, A.R. Yavari^{a, b, c}

^a SIMaP, CNRS UMR 5266, Grenoble University – Institut Polytechnique, BP. 75, St-Martin d'Herès 38402, France

^b DEMa, Universidade Federal de São Carlos – UFSCar, SP, São Carlos 13565-905, Brazil

^c WPI Advanced Institute for Materials Research, Tohoku University, Sendai 980-8577, Japan

ARTICLE INFO

Article history:

Received 23 July 2015

Received in revised form

27 September 2015

Accepted 30 September 2015

Available online 9 October 2015

Keywords:

Phase separation

Nanostructures

Nanoporous

Titanium alloys

Phase transformation

ABSTRACT

Porous noble metal surfaces were produced by gold-smiths in ancient times by dealloying. These processes lead to the formation of gold or other noble metal rich layers. Such dealloying occurs by corrosion as the most electro-chemically active elements dissolve and the more noble elements aggregate into clusters by phase separation (spinodal decomposition). Here we report results from an alternative path to nanoporosity where the structure patterns and length scales are first fixed in the bulk by high-temperature spinodal decomposition followed by chemical dissolution of one of the component products of the phase-separation. The process may be used to form nanoporous titanium for biochemical applications.

© 2015 Elsevier Inc. All rights reserved.

1. Introduction

To understand nanoporous noble metal formation by dealloying, Erlebacher et al. [1] proposed a continuum model with experimental and Monte Carlo simulation evidence for an intrinsic dynamical structure pattern formation. The pores form as the more noble elements aggregate into clusters by phase separation (spinodal decomposition). According to these authors, a multi-scale model including the kinetics of selective dissolution, surface diffusion, and mass transport through the bulk of the growing phase is needed for the full understanding of development of such nanoporosity.

Starting with an alternative path-way, we use controlled high-temperature phase-separation in a binary Ti-rich alloy to first fix the length-scale of the nanostructure. This phase-separated nanostructure constituted of Ti-rich and Ti-poor regions on the scale of half the spinodal wavelength λ_s is subsequently chemically treated to obtain micro- and nanoporous titanium on a pre-determined scale $\lambda_s/2$. These processes can lead to functional geometries of nanoporous metals with interconnected voids and large surface to volume ratios. The geometries include bulk nanostructured materials the outer-surface of which have been rendered micro- and

nanoporous as well as foils and films of nanostructured materials rendered micro- and nanoporous across the thickness with communicating nano-voids.

Biocompatibility, corrosion resistance, specific strength [2–4] and Young's modulus closer to those of bones place titanium and its alloys among the most appropriate materials for orthopedics, bone plates, vascular grafts and dental implants [5,6]. However, Young's modulus of Ti (105 GPa) [2] needs to be brought closer to those of various bones (about 20 GPa) to minimize “stress shielding” which is the main cause of bone resorption and implant loosening [7–9]. Increased porosity proportionally lowers Young's modulus [10] and a rough micro or nanoporous surface increases total bone contact surface leading to improved strength of bone-implant fixation [11].

Such pores may also be loaded with stored bioactive compounds (e.g. proteins and antibiotics) for slow release [12] such that nano-micro porous networks can act as reservoirs for bioactive compounds or antibacterial drugs, preventing infections and inflammations that can lead to septic loosening of implants [13] during healing.

2. Experimental

Pure titanium and scandium elements (purity 99.98% and 99.9%, respectively) were melted together in an arc-furnace under argon

* Corresponding author. 1130 rue de la Piscine, 38402 Saint-Martin d'Herès, France.

E-mail address: [ntpnanag@simap.grenoble-inp.fr](mailto:ntpanag@simap.grenoble-inp.fr) (N.T. Panagiotopoulos).

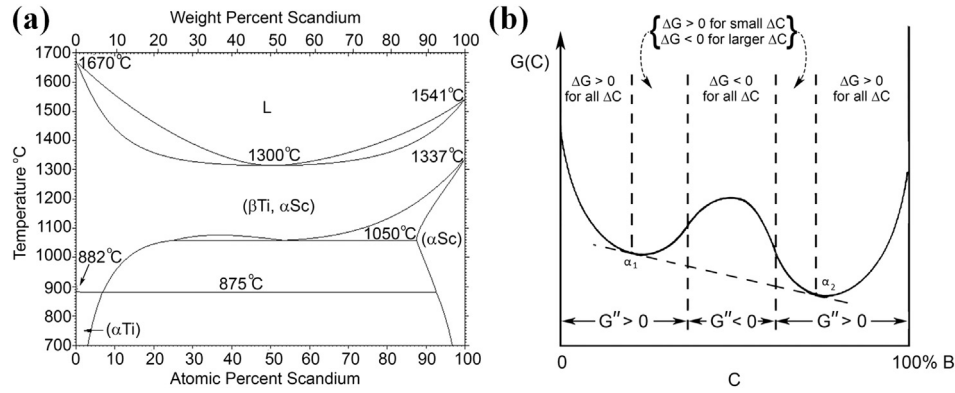


Fig. 1. Spinodal decomposition. a) Titanium–Scandium binary phase-diagram with miscibility gap and decomposition below about 1350 K (near 1080 °C). b) Schematic drawing of the spinodal decomposition range where the second composition derivative $G''(c) < 0$.

atmosphere to prepare bulk Ti–Sc as a model system. The alloys were re-melted at least 5 times to ensure compositional homogeneity. Thin foils were prepared by rapid re-solidification of the bulk Ti–Sc alloys using a single copper roller melt-spinning technique.

The microstructure of the Ti–Sc alloys was revealed by chemical etching with a nitric acid (HNO_3) solution. A hydrofluoric acid (HF) solution was used for chemical etching of pure Ti foils for comparison as HNO_3 did not attack pure Ti; titanium exhibits excellent corrosion resistance to HNO_3 at room temperature [14].

The surface of Ti–Sc alloys after etching has been observed using a ZEISS ULTRA 55 FEG scanning electron microscope (FEG-SEM) operated at 3 KeV using an in-lens secondary electron (SE) detector reaching a resolution of ~ 1 nm. Chemical analysis was carried out by a Bruker AXS X-ray energy dispersive spectrometer (EDX) coupled to the FEG-SEM using an excitation electron beam of 10 KeV.

Porosity in Ti–Sc bulk alloys and foils was induced by simple immersion in (70%) HNO_3 solution for different leaching times at room temperature followed by rinsing with de-ionized water. Porosity was measured by image analysis on high-resolution SEM micrographs (ImageJ software [15]) from at least 10 surface regions, and by density measurements compensated for the Sc loss.

The structural characterization of nanoporous titanium was performed by a Panalytical X'Pert Pro X-ray diffractometer (XRD) with Cu K_α radiation.

3. Results and discussion

Through the wavelength of spinodal decomposition λ_s , it is possible to generate controlled nanostructures but Ti is a rather reactive metal and Ti-alloy solid-state miscibility gaps are rare.

One such system is the titanium-scandium binary as can be seen in the ASM phase-diagram below (Fig. 1a). Phase diagrams are established by a combination of calculations and experimental data in order to obtain the free energy $G(c)$ curves of different phases at various temperatures. The schematic drawing (Fig. 1b) from Shewmon [16] is typical of A_1 - cB_c binary system that undergoes spinodal decomposition. As in the drawing, the spinodal range is where the second composition derivative $G''(c) < 0$.

Fig. 2 shows SEM images of a pure (commercial) Ti foil and the as-prepared Ti–Sc bulk alloy after etching. It can be seen that while pure Ti is only attacked on the grain-boundaries of its μm -scale structure, the bulk alloy which spinodally decomposes during cooling has been deeply attacked (the voids are black) along the Sc-rich part of the decomposition wavelength $\lambda_s \approx 150$ nm.

The present experiment demonstrates a practical pathway to nanoporous Ti alloy surfaces.

Spinodal decomposition was given a quantitative basis in the 1950s and 1960s by Hilliard, Cahn and Hilliard [17]. It can be shown that for an approximately 50/50 solution with the gradient energy $K \sim (2/3) \cdot \Delta H_{\text{mix}} \cdot r_0^2$ where $2r_0$ is the average interatomic distance and ΔH_{mix} is the heat of mixing, the critical spinodal wavelength λ_c can be approximately calculated as [17,18].

$$\lambda_c = 4(2/3)^{1/2} \pi r_0 \cdot \Delta H_{\text{mix}}^{1/2} / \left(R(T_{\text{spinodal}} - T) \right)^{1/2} \quad (1)$$

where R is the gas constant.

Taking a nanostructure spinodally decomposed around $T_{\text{spinodal}} - T \approx 10$ K during solidification, with $2r_0 \approx 3 \cdot 10^{-8}$ cm, Miedema's [19] value for $\Delta H_{\text{mix}} \approx +10$ kJ mol $^{-1}$ and $R = 8.314$ J mol $^{-1}$ K $^{-1}$, one obtains $\lambda_c \approx 17$ nm.

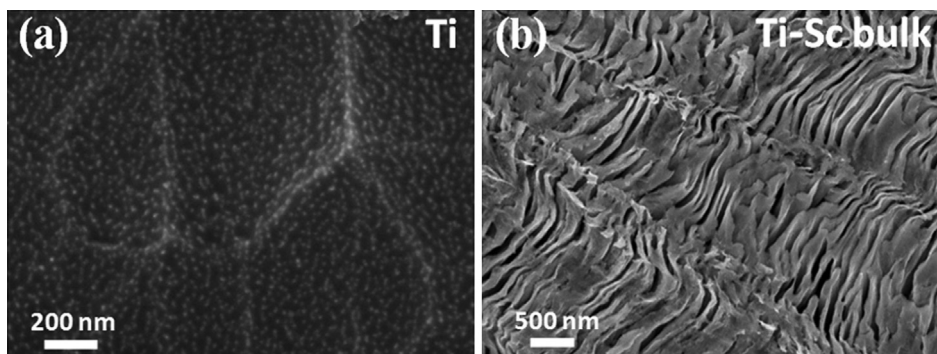


Fig. 2. Scanning electron micrographs after etching of a) pure Ti and b) bulk Ti–Sc ingot.

Download English Version:

<https://daneshyari.com/en/article/72027>

Download Persian Version:

<https://daneshyari.com/article/72027>

[Daneshyari.com](https://daneshyari.com)